Quantitative Comparison of the Microscopic Anatomy of the Human ACL Femoral and Tibial Entheses

Mélanie L. Beaulieu,[1,4] Grace E. Carey,[1,4] Stephen H. Schlecht,[2] Edward M. Wojtys,[2,3] James A. Ashton-Miller[1,4]

[1]School of Kinesiology, University of Michigan, Ann Arbor, Michigan, [2]Department of Orthopaedic Surgery, University of Michigan, Ann Arbor, Michigan, [3]MedSport, University of Michigan, Ann Arbor, Michigan, [4]Biomechanics Research Laboratory, Department of Mechanical Engineering, University of Michigan, Ann Arbor, Michigan

ABSTRACT: The femoral enthesis of the human anterior cruciate ligament (ACL) is known to be more susceptible to injury than the tibial enthesis. To determine whether anatomic differences might help explain this difference, we quantified the microscopic appearance of both entheses in 15 unembalmed knee specimens using light microscopy, toluidine blue stain and image analysis. The amount of calcified fibrocartilage and uncalcified fibrocartilage, and the ligament entheseal attachment angle were then compared between the femoral and tibial entheses via linear mixed-effects models. The results showed marked differences in anatomy between the two entheses. The femoral enthesis exhibited a 3.9-fold more acute ligament attachment angle than the tibial enthesis ($p < 0.001$), a 43% greater calcified fibrocartilage tissue area ($p < 0.001$), and a 226% greater uncalcified fibrocartilage depth ($p < 0.001$), with the latter differences being particularly pronounced in the central region. We conclude that the ACL femoral enthesis has more fibrocartilage and a more acute ligament attachment angle than the tibial enthesis, which provides insight into why it is more vulnerable to failure. © 2015 Orthopaedic Research Society. Published by Wiley Periodicals, Inc. J Orthop Res 33:1811–1817, 2015.

Keywords: anterior cruciate ligament; enthesis; histology; anatomy; fibrocartilage

Injuries to the anterior cruciate ligament (ACL) pose extensive health and financial difficulties, both short- and long-term.[1,2] The majority of ACL ruptures occur near its femoral origin or "enthesis,"[3–5] rather than elsewhere, but the underlying reason for this remains unknown. We speculate that the anatomy of the ACL femoral enthesis may be significantly different than the tibial enthesis, which may be indicative of heterogeneous forces applied at, and near, the entheses.[6–8] If confirmed, it might help explain the higher failure rate at, or near, the femoral enthesis.

The microscopic anatomy of ligament and tendon entheses minimizes stress concentrations and distributes forces across the entire attachment area.[9,10] Entheses are classified as either fibrous or fibrocartilaginous according to the type of tissue comprising the attachment site.[10] Fibrocartilaginous entheses are characterized by four zones of tissue: dense fibrous connective tissue, uncalcified fibrocartilage (UF), calcified fibrocartilage (CF), and bone.[10] The quantity of each tissue type is characteristic of the mechanical loading at the enthesis.[6–8] For example, the quantity of UF has been positively related to the change in angle that occurs between the ligament/tendon and the bone to which it attaches during joint motion;[6,7] while the quantity of cortical calcified tissue has been positively related to the size of the ligament/tendon, and thus the tensile force applied to the bone.[6,8] Most fibrocartilaginous entheses, however, do not contain fibrocartilage across the entire attachment site, with the superficial portions frequently being more fibrous.[10]

Descriptions of the ACL entheses have mostly focused on their macroscopic characteristics and dimensions.[11,12] Few studies have explored these entheses at a microscopic level, and those that have, focused on the femoral enthesis.[13–17] Arnoczky characterized the ACL entheses as fibrocartilaginous, with a description of the transitional zones of UF and CF.[14] Tissue quantification has not been reported for UF, either at the femoral or the tibial entheses. Greater UF may be expected at the femoral enthesis than the tibial enthesis given the greater change in ACL-bone angle reported at the femur during passive knee flexion.[18]

Lastly, the oblique angle at which a tendon/ligament attaches to the bone has been shown, by computer simulations, to induce a strain concentration where the shortest longitudinal fibers of the tendon/ligament originate from, or insert into, bone at the enthesis.[19,20] And that strain concentration increased with more acute attachment angles.[19] It is unknown, however, whether the femoral ACL entheseal attachment angle is more acute than the tibial attachment angle, thereby inducing greater strain concentration at the femur.

The purpose of this study was to quantify and compare the microscopic anatomy of the human ACL femoral and tibial entheses by means of histological analyses. We tested the primary null hypothesis that there would be no difference in relative area of CF, or the average depth of UF, between the femoral and tibial entheses. We also tested the secondary null hypothesis that there would be no difference between the femoral and tibial ACL entheseal attachment angles.

METHODS

Specimen Procurement and Preparation
Fifteen unembalmed human knee specimens, including seven pairs, were harvested from four male and four female donors (age $= 52.1 \pm 8.4$ years; height $= 1.70 \pm 0.10$ m; mass $= 70.5 \pm 15.9$ kg; BMI $= 24.1 \pm 4.3$ kg/m^2) through the

University of Michigan Anatomical Donations Program for this cross-sectional study of Level of Evidence 3. All specimens were dissected so as to leave only the ACL, distal femur, and proximal tibia. No macroscopic evidence of previous ACL injury was observed in the dissected specimens. The femur-ACL-tibia complexes were fixed in 10% neutral buffered formalin for 48 h, with the knee in 15° of flexion, 0° of abduction/adduction, and 0° of axial rotation as measured with a goniometer placed along the anatomical axes of the tibia and femur, by means of a custom-built fixation device, to maintain the ligament's natural twist and angle of attachment to each bone. Then, two smaller samples were cut from each femur-ACL-tibia complex for histochemical processing (Table 1): the ACL-femur and ACL-tibia attachment sites. Once processed and embedded in methyl methacrylate, tissue samples were sectioned using a commercially available precision sectioning saw (IsoMet[TM] Low Speed Saw, Buehler, Lake Bluff, IL). For each tissue sample, four thick sections were extracted, mounted on a slide, ground, and polished (EcoMet[TM] 300 Pro-Grinder/Polisher, Buehler, Lake Bluff, IL) to obtain tissue sections of approximately 100 μm in thickness. Tibial tissue samples were sectioned in a parasagittal plane. Femoral samples were sectioned along the longitudinal axis of the ACL, with both tissue samples sectioned at 20%, 40%, 60%, and 80% of the width of the enthesis (Fig. 1). The mounted sections were surface

Table 1. Tissue Processing Protocol for Histological Analysis

Solution	Time (h)
Defat	
Ethanol:ether (1:1)	8
Chloroform:methanol (2:1)	16
Rinse	
Chloroform	1
Chloroform	1
Ethylene glycol monoethyl ether	12
Dehydration	
Ethylene glycol monoethyl ether	8
Ethylene glycol monoethyl ether	8
Ethylene glycol monoethyl ether	8
Ethylene glycol monoethyl ether	8
Rinse	
2-propanol	8
2-propanol	8
2-propanol	8
Clear	
Methyl salicylate	8
Methyl salicylate	8
Process	
Methyl methacrylate I[a]	24
Clear	
Methyl methacrylate I[a]	96
Methyl methacrylate II[b]	96
Methyl methacrylate III[b]	96
Embed	
Methyl methacrylate IV[b]	~432

[a]Methyl methacrylate (MMA) and n-butyl phthalate.[b]MMA, n-butyl phthalate, and dry benzoyl peroxide (varying amounts of benzoyl peroxide in MMA II-IV).

stained with toluidine blue for light microscopy viewing. High resolution digital images (4,000 dpi) of all sections were obtained with a film scanner (Nikon Super CoolScan 5000ED) for further analyses.

Quantitative Analysis

From the digital images of tissue sections, the diameters of the femoral and tibial entheses were measured and averaged over all four sections. The diameter was defined as the linear distance between the edges of the enthesis (Fig. 2A). The relative area of CF was also quantified by outlining this tissue using a pen display (Cintiq 24HD w/grip pen, Wacomb, Kazo, Saitama, Japan) and dividing this area by the length of the enthesis, defined as the length of the profile of the tidemark (Fig. 2B). We measured CF relative area because the area measurement includes all CF in the enthesis rather than a sampling of its depth at discrete intervals. In addition, the depth of UF was measured at 500 μm intervals along the entire enthesis (Fig. 2C). A sample of depth was selected here as the quantification method because the interface between the UF and the dense fibrous connective tissue was less apparent than for the CF, making a relative area measurement impractical (Fig. 2B and C). Also, sampling UF depth at a constant interval has been used previously to quantify UF in human quadriceps tendons and patellar ligaments.[7] This variable was defined as the perpendicular distance from the tidemark to the end of the UF tissue, delineated by the furthest chondrocyte[7] viewed with a light microscope (BX-51, Olympus, Center Valley, PA) at ×100 and ×400 magnifications (Fig. 2C). Finally, the ligament entheseal attachment angle, defined as the angle between a line parallel to the fibers of the dense fibrous connective tissue and a line of best fit to the entheseal surface (i.e., tidemark), was measured in each tissue section (Fig. 2D). This line of best fit was obtained by digitizing the tidemark and fitting a first order (linear) polynomial curve to the digitized points. All measurements were made in ImageJ.[21] CF relative area was quantified over the diameter of the enthesis, as well as for the middle 50% and outer 50% of the enthesis diameter (Fig. 2A), and averaged over all four tissue sections. UF depth was averaged over the diameter of the enthesis, as well as over the middle 50% and outer 50% of the diameter of the enthesis, and then averaged over all sections. These data were averaged over all sections and compared between regions (middle and outer) based on previous ACL histological work revealing qualitative difference in CF between similar regions in the femoral enthesis.[15–17] The entheseal attachment angle was averaged over all sections. The intraclass correlation coefficients (ICC) for the measurements were 0.98 for CF relative area, 0.83 for the UF depth, and 0.99 for the ligament entheseal angle.
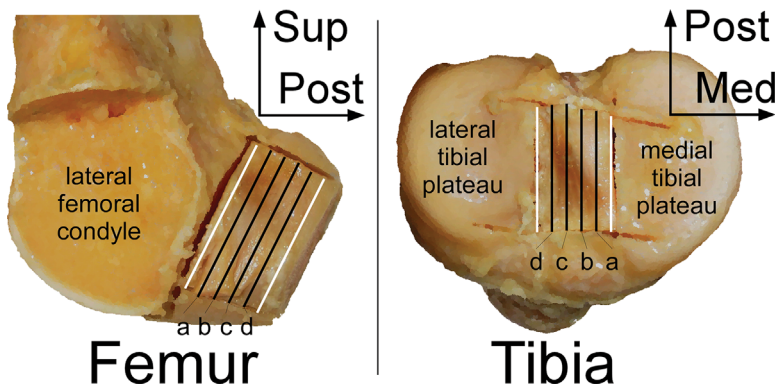
Statistical Analysis

The hypotheses were statistically tested by means of a series of linear mixed-effects models with CF relative area, UF depth, and entheseal attachment angle as the outcome variables and enthesis (coded as "1" = femur and "2" = tibia), knee specimen, and knee donor as the predictor variables. A second series of linear mixed-effects models were run to gain further insight on quantitative differences between femoral and tibial entheses. For these models, CF relative area and UF depth were the outcome variables and enthesis region

Figure 1. Location of tissue sections (black lines) prepared for histological analysis on the femoral and tibial tissue blocks of a right knee specimen. White lines indicate the edges of the entheses. a: 20%; b: 40%; c: 60%; d: 80% of the width of the enthesis.

(coded as "1" = middle 50% of femoral enthesis, "2" = outer 50% of femoral enthesis, "3" = middle 50% of tibia enthesis, and "4" = outer 50% of tibia enthesis), knee specimen, and knee donor were the predictor variables. Knee donor was included in the models to account for the correlation between specimens harvested from the same donor. Additionally, the average diameter of the femoral and tibial entheses were compared with a linear mixed-effects model with diameter as the outcome variable and the same predictor variables as described above for the first series of models. An alpha level below 0.05 indicated statistical significance.

RESULTS
Qualitative Analysis
The femoral entheses were fibrocartilaginous in that they comprised four distinct zones of tissue: dense fibrous connective tissue, UF, CF, and bone (Fig. 3A–D and I). The periphery, especially the most superior and posterior regions, however, contained little or no fibrocartilage. The superior fibers were found to extend to, and blend into, the posterior articular cartilage (Fig. 3J); the inferior fibers originated adjacent to the lateral intercondylar ridge. The shape of the femoral enthesis was generally convex in the most anterior section (section "a" in Fig. 1 and Fig. 3A), but generally concave in the most posterior section (section "d" in Fig. 1 and

Fig. 3D), and more complex in the middle sections (Fig. 3B and C). Finally, in the regions with a large quantity of UF, typically the middle to inferior one-third of the enthesis, the fibrocartilage transitioned from calcified to uncalcified, and thus arose from the tidemark, at a less acute angle and curved to align with the primary collagen fiber direction of the ligament (Fig. 3I).

The tibial entheses were also fibrocartilaginous, but with smaller and relatively uniform quantities of fibrocartilage across the enthesis in comparison with the femoral entheses (Fig. 3E–H and K). They inserted into a bony depression delineated anteriorly by the anterior ridge and posteriorly by the anterior intertubercular fossa. In comparison with the femoral enthesis, the trabecular bone appeared to be more anisotropic (Fig. 3A–H).

Quantitative Analysis
The mean entheseal diameters, averaged over all sections of the femoral and tibial entheses, were 14.8 ± 3.2 mm and 15.8 ± 2.0 mm, respectively ($p = 0.140$). Overall, the relative area of CF and average depth of UF were 43% and 226% greater at the femoral enthesis than the tibial enthesis, respectively ($ps < 0.001$) (Fig. 4A and B). Additional region-specific comparisons revealed that this difference in
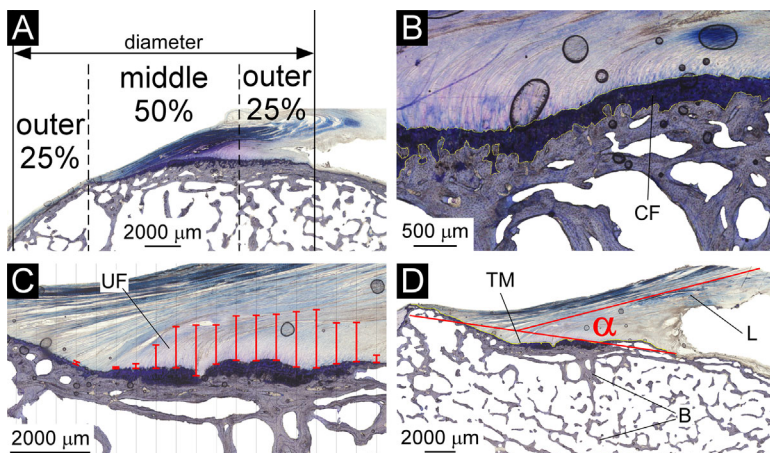
Figure 2. (A) Definition of the diameter of the enthesis and of the enthesis regions for which the dependent variables were quantified. Example of the (B) outline of CF area, (C) UF depth measured at 500 μm intervals, and (D) ligament entheseal attachment angle measurement. cf: calcified fibrocartilage; uf: uncalcified fibrocartilage; tm: tidemark; b: bone; l: ligament. Toluidine blue strain.
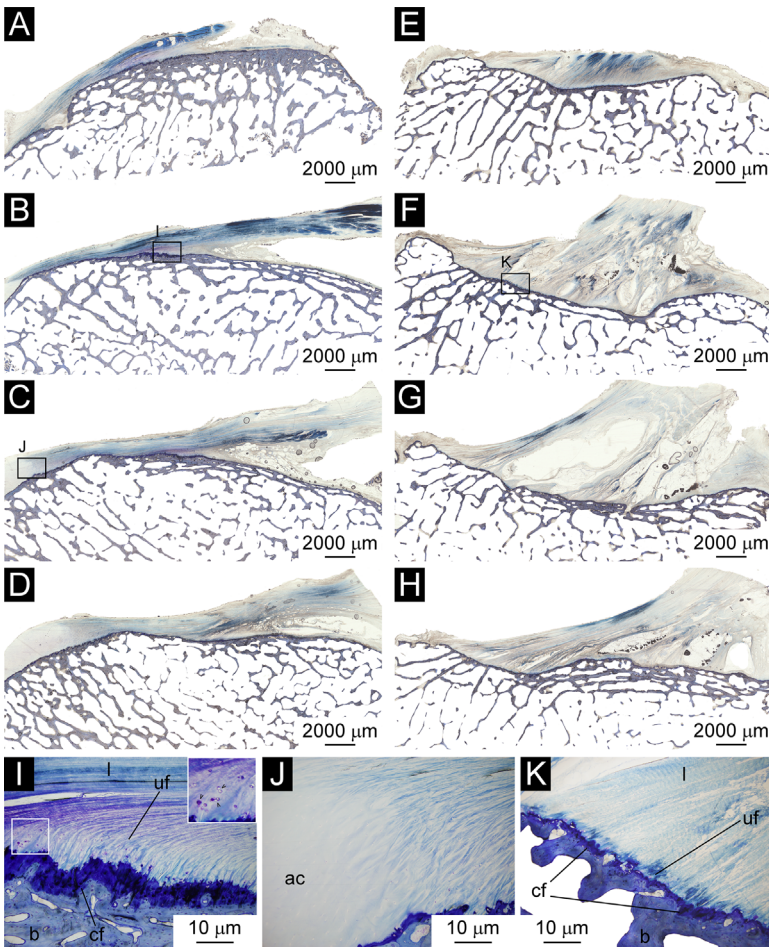
Figure 3. Histology of the four tissue sections of the ACL femoral (A: 20%; B: 40%; C: 60%; D: 80% of the width of the enthesis) and tibial (E: 20%; F: 40%; G: 60%; H: 80% of the width of the enthesis) entheses in a representative specimen in terms of fibrocartilage quantity, entheseal surface shape, and ligament entheseal attachment angle. The large voids in the tibia may be fat deposits. (I) Femoral entheses had four zones of tissue: ligamentous tissue (l), uncalcified fibrocartilage (uf), calcified fibrocartilage (cf), and bone (b). Note how the ligamentous tissue transitions into uncalcified fibrocartilage and curves to insert into the calcified tissue at a less acute angle. Inset: High power view of tissue outlined in white showing uncalcified fibrocartilage with its fibrocartilage cells (arrow heads). (J) The femoral enthesis often extended to, and blended into, the posterior articular cartilage (ac). (K) Tibial entheses also had four zones of tissue, but with less fibrocartilage. Toluidine blue stain.

CF relative area between entheses was significant only in the middle 50% of the enthesis ($p < 0.001$) (Fig. 4A). Furthermore, the difference in average UF depth between the femoral and tibial entheses was significant in the middle 50% ($p < 0.001$) as well as the outer 50% of the enthesis ($p = 0.009$) (Fig. 4B). As for the entheseal attachment angle, it was 3.9 times smaller at the femoral enthesis compared with the tibial enthesis ($p < 0.001$) (Fig. 4C).

DISCUSSION

The goal of this study was to compare the microscopic anatomy of the ACL tibial and femoral entheses. Our histological analyses revealed significant differences in the quantity of fibrocartilage, and especially the angle at which the ACL attaches to the bone (i.e., the "entheseal attachment angle") at the femoral and tibial entheses. When these anatomic differences are interpreted in a biomechanical context, they help
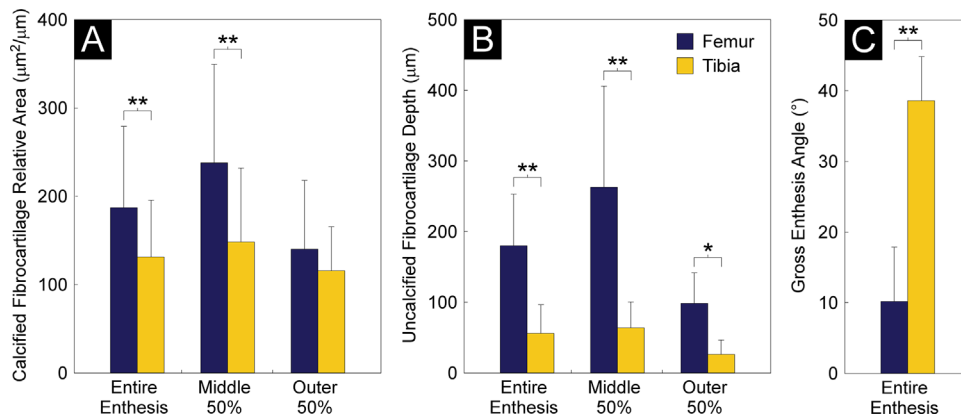
Figure 4. Mean and standard deviation of (A) relative area of calcified fibrocartilage and (B) depth of uncalcified fibrocartilage of all tissue sections for the entire enthesis and by region, as well as (C) ligament entheseal attachment angle of all tissue sections for the entire enthesis presented for the femoral and tibial entheses. *Significantly different, $p < 0.01$; **significantly different, $p < 0.001$.

provide new insight into why the femoral enthesis is more vulnerable to failure.

The primary null hypothesis was rejected because more CF and UF were found at the femoral enthesis, especially in its middle region. Although the ACL entheses have been the subject of several histological analyses,[13–17] we were unable to find quantitative comparisons of femoral and tibial entheseal anatomy. The only other study to quantify fibrocartilage did so at the femoral enthesis and measured the combined depth of the calcified fibrocartilage and subchondral bone (CFB).[16] We also made this measurement, but did not present those data to avoid redundancy, given similar trends in CF relative area and CFB depth. Therefore, our results corroborate those of Sasaki;[16] qualitatively more calcified tissue appears to be present in the central region of the femoral enthesis in both studies.

The magnitude of UF and CF at an enthesis has been proposed to be positively related to the change in angle between the ligament and the bone to which it attaches and to the tensile force applied to the bone, respectively.[6–8] It is not surprising, therefore, that more UF was present at the femoral enthesis than at the tibial enthesis given the greater change in ACL-bone angle at the femoral enthesis measured in vitro during passive knee flexion.[18] Specifically, the ACL-femur angle increases 54° during knee flexion (0–140°), on average, in comparison with the ACL-tibia angle, which only decreases an average of 23°.[18] The greater quantity of UF at the femoral enthesis, therefore, may help reduce bending moments at the enthesis calcified-uncalcified junction.[22] As for the CF, its greater quantity at the femoral enthesis may indicate greater stress there than at the tibia, as suggested by Evans et al.[8] Assuming that the load magnitude applied to the enthesis is the same at the femoral and tibial attachments of a given ACL, we speculate that the larger footprint of the tibial enthesis[23] and the concavity into which it inserts, which lengthens the entheseal "bond" between soft and hard tissue, reduces the average tensile stress (i.e., force per unit area) at the tibial enthesis. Hence, less CF may be required at the tibial enthesis in comparison with the femoral enthesis. Benjamin et al.,[10] on the other hand, suggested that less calcified tissue (CF and subchondral bone) allows for greater deformation of the enthesis, and thus greater dissipation of energy. They have also proposed that the lateral tibial spine reduces stress at the tibial enthesis by allowing the ACL to bend over it, as the spine acts like a pulley.[24] However, we did not observe such bending in our specimens. Perhaps this is only a factor at greater angles of knee flexion, given that the angle at which the ACL inserts into the tibia decreases with knee flexion[18]. All our knee specimens were fixed at 15° of flexion—the mean knee flexion angle at initial contact during ACL injury scenarios,[25] and that used for

in vitro studies.[26] The angle at which the ACL-bone specimens were fixed by Benjamin et al., however, was not reported.[24] Even though it appears to be dimensioned appropriately (i.e., more CF), the smaller femoral enthesis is systematically loaded by a greater average tensile stress than the tibial enthesis. It is logical, therefore, that it could accumulate microdamage over time, especially given recent evidence that the ACL is indeed susceptible to fatigue failure.[5,27]

We rejected the secondary null hypothesis in that the ACL was found to arise from the femur at a nearly fourfold more acute angle than it inserts into the tibia. Zaffagnini et al.[18] also examined ACL-bone angles, but they did not use a plane representative of the entheseal surface (or "tidemark"). Rather, they used a plane that was representative of the articular surface of the bones to calculate these angles. From a biomechanical viewpoint, the more acute femoral entheseal angle will induce a greater strain concentration at the inferior margin of the femoral enthesis than at the tibial enthesis, based on in silico evidence.[19] In a two-dimensional finite element model of the puboviseral muscle and its enthesis, an inverse relation was found between enthesis angle and strain energy concentration: the smaller the attachment angle, the greater the strain concentration.[19] The more acute entheseal attachment angle at the femur and the putative greater strain concentration may partly explain the greater quantity of CF, in comparison with tibial enthesis. It might help explain why the ACL often fails at, or near, the femoral enthesis.

We note several limitations of this study. First, we used older specimens (age $= 52.1 \pm 8.4$ years) to gain insight on an injury that mainly occurs in adolescents and young adults.[28] Fibrocartilaginous entheses are known to be affected by age-related degenerative changes, such as microdamage and an increase in thickness of the CF.[29] There is no evidence that these changes would affect the femoral and tibial entheses differently, so the general qualitative trends should remain valid. Second, the donors' history of physical activity was unknown; certain activities could have induced entheseal trauma and microtrauma, thereby producing architectural changes at the enthesis.[30] Without a detailed history, however, we cannot interpret with confidence any variations/abnormalities. Third, three potential sources of error in the measurement of the ligament entheseal attachment angle exist. (1) The method used to measure the ligament entheseal attachment angle was not entirely objective given that the line parallel to the fibers of the dense fibrous connective tissue was identified visually. (2) Although every effort was made to consistently section our samples in the same plane, between-samples variability most likely existed. (3) The angle of a three-dimensional structure was estimated from two-dimensional images.

Given the excellent reliability (ICC = 0.99) of this method and the nearly fourfold difference in angle between the tibial and femoral entheses, however, we believe the effect of these sources of error to be minimal on our results. Future entheseal morphology work should use a three-dimensional approach (e.g., micro-CT) to examine the ligament attachment angle and compare results to our two-dimensional method.

In summary, more fibrocartilage tissue was found at the femoral enthesis than at the tibial enthesis. Furthermore, the ACL was found to arise from the femur at a significantly more acute angle than that at which it inserts into the tibia. It is possible that these differences may induce a strain concentration at the inferior margin of the ACL's femoral enthesis, thus making this region susceptible to damage accumulation.

AUTHORS' CONTRIBUTIONS

MLB made substantial contributions to the study design, the acquisition, analysis and interpretation of the data, and the drafting and critical revising of the manuscript. GEC made substantial contributions to the acquisition and analysis of the data. SHS made substantial contributions to the study design, the acquisition and interpretation of the data and the critical revising of the manuscript. EMW made substantial contributions to the study design, the interpretation of the data, and the critical revising of the manuscript. JAM made substantial contributions to the study design, the interpretation of the data, and the drafting and critical revising of the manuscript. All authors have read and approved the final submitted manuscript.

ACKNOWLEDGMENTS

REFERENCES

1. Lohmander LS,Englund PM, Dahl LL, et al. 2007. The long-term consequence of anterior cruciate ligament and meniscus injuries: osteoarthritis. Am J Sports Med 35:1756–1769.
2. Riordan EA, Frobell RB, Roemer FW, et al. 2013. The health and structural consequences of acute knee injuries involving rupture of the anterior cruciate ligament. Rheum Dis Clin North Am 39:107–122.
3. Meyer EG, Baumer TG, Slade JM, et al. 2008. Tibiofemoral contact pressures and osteochondral microtrauma during anterior cruciate ligament rupture due to excessive compressive loading and internal torque of the human knee. Am J Sports Med 36:1966–1977.
4. Zantop T, Brucker PU, Vidal A, et al. 2007. Intraarticular rupture pattern of the ACL. Clin Orthop Relat Res 454:48–53.
5. Lipps DB, Wojtys EM, Ashton-Miller JA. 2013. Anterior cruciate ligament fatigue failures in knees subjected to repeated simulated pivot landings. Am J Sports Med 41:1058–1066.
6. Benjamin M, Evans EJ, Rao RD, et al. 1991. Quantitative differences in the histology of the attachment zones of the meniscal horns in the knee joint of man. J Anat 177:127–134.
7. Evans EJ, Benjamin M, Pemberton DJ. 1990. Fibrocartilage in the attachment zones of the quadriceps tendon and patellar ligament of man. J Anat 171:155–162.
8. Evans EJ, Benjamin M, Pemberton DJ. 1991. Variations in the amount of calcified tissue at the attachments of the quadriceps tendon and patellar ligament in man. J Anat 174:145–151.
9. Schlecht SH. 2012. Understanding entheses: bridging the gap between clinical and anthropological perspectives. Anat Rec (Hoboken) 295:1239–1251.
10. Benjamin M, Kumai T, Milz S, et al. 2002. The skeletal attachment of tendons-tendon "entheses". Comp Biochem Physiol A Mol Integr Physiol 133:931–945.
11. Ferretti M, Doca D, Ingham SM, et al. 2012. Bony and soft tissue landmarks of the ACL tibial insertion site: an anatomical study. Knee Surg Sports Traumatol Arthrosc 20:62–68.
12. Otsubo H, Shino K, Suzuki D, et al. 2012. The arrangement and the attachment areas of three ACL bundles. Knee Surg Sports Traumatol Arthrosc 20:127–134.
13. Tensho K, Shimodaira H, Aoki T, et al. 2014. Bony landmarks of the anterior cruciate ligament tibial footprint: a detailed analysis comparing 3-dimensional computed tomography images to visual and histological evaluations. Am J Sports Med 42:1433–1440.
14. Arnoczky SP. 1983. Anatomy of the anterior cruciate ligament. Clin Orthop Relat Res 19–25.
15. Iwahashi T, Shino K, Nakata K, et al. 2010. Direct anterior cruciate ligament insertion to the femur assessed by histology and 3-dimensional volume-rendered computed tomography. Arthroscopy 26:S13–S20.
16. Sasaki N, Ishibashi Y, Tsuda E, et al. 2012. The femoral insertion of the anterior cruciate ligament: discrepancy between macroscopic and histological observations. Arthroscopy 28:1135–1146.
17. Mochizuki T, Fujishiro H, Nimura A, et al. 2014. Anatomic and histologic analysis of the mid-substance and fan-like extension fibres of the anterior cruciate ligament during knee motion, with special reference to the femoral attachment. Knee Surg Sports Traumatol Arthrosc 22:336–344.
18. Zaffagnini S, Martelli S, Acquaroli F. 2004. Computer investigation of ACL orientation during passive range of motion. Comput Biol Med 34:153–163.
19. Kim J, DeLancey JO, Ashton-Miller JA. 2011. Why does the pubovisceral muscle fail at its enthesis, and not elsewhere, during the second stage of labor? A computational study. Presented at the Annual Meeting of the American Society of Biomechanics. Aug 10–13. Long Beach, CA, USA.
20. Oh YK, Beaulieu ML, Lipps DB, et al. 2013. Is the strain concentration at the femoral enthesis a risk factor for anterior cruciate ligament injury? Presented at the Annual Meeting of the American Society of Biomechanics. Sept 4–7. Omaha, NE, USA.
21. Schneider CA, Rasband WS, Eliceiri KW. 2012. NIH Image to ImageJ: 25 years of image analysis. Nat Methods 9:671–675.
22. Benjamin M, McGonagle D. 2001. The anatomical basis for disease localisation in seronegative spondyloarthropathy at entheses and related sites. J Anat 199:503–526.
23. Iriuchishima T, Shirakura K, Yorifuji H, et al. 2013. ACL footprint size is correlated with the height and area of the lateral wall of femoral intercondylar notch. Knee Surg Sports Traumatol Arthrosc 21:789–796.
24. Benjamin M, Moriggl B, Brenner E, et al. 2004. The "enthesis organ" concept: why enthesopathies may not

present as focal insertional disorders. Arthritis Rheum 50:3306–3313.

25. Krosshaug T, Nakamae A, Boden BP, et al. 2007. Mechanisms of anterior cruciate ligament injury in basketball: video analysis of 39 cases. Am J Sports Med 35:359–367.

26. Beaulieu ML, Oh YK, Bedi A, et al. 2014. Does limited internal femoral rotation increase peak anterior cruciate ligament strain during a simulated pivot landing? Am J Sports Med 42:2955–2963.

27. Beaulieu ML, Wojtys EM, Ashton-Miller JA. 2015. Risk of ACL fatigue failure is increased by limited internal femoral rotation during in vitro repeated pivot landings. Am J Sports Med In print. DOI: 10.1177/0363546515589164

28. Kobayashi H, Kanamura T, Koshida S, et al. 2010. Mechanisms of the anterior cruciate ligament injury in sports activities: a twenty-year clinical research of 1,700 athletes. J Sports Sci Med 9:669–675.

29. Villotte S, Knüsel CJ. 2013. Understanding entheseal changes: definition and life course changes. Int J Osteoarchaeol 23:135–146.

30. Resnick D, Niwayama G. 1983. Entheses and enthesopathy. Anatomical, pathological, and radiological correlation. Radiology 146:1–9.